EXAFS, EPR, and Electronic Absorption Spectroscopic Study of the α Metallosubunit of CO Dehydrogenase from *Clostridium thermoaceticum*

Jinqiang Xia,[†] Jun Dong,[‡] Shengke Wang,[‡,§] Robert A. Scott,*[,‡] and Paul A. Lindahl*[,†]

Contribution from the Department of Chemistry, Texas A & M University, College Station, Texas 77843, and Center for Metalloenzyme Studies, University of Georgia, Athens, Georgia 30602

Received March 1, 1995[⊗]

Abstract: The α metallosubunit of carbon monoxide dehydrogenase from *Clostridium thermoaceticum* was isolated by subjecting native enzyme to low concentrations of the detergent sodium dodecyl sulfate, followed by anaerobic preparative native polyacrylamide gel electrophoresis. The isolated α subunit absorbs in the 400 nm region and contains one Ni and four Fe ions. The irons are organized into an $[Fe_4S_4]^{2+/1+}$ cluster, the reduced form of which exhibits EPR features between g = 6 and 3, and a weak (0.1 spin/α) $g_{av} = 1.94$ signal. The reduced cluster appears to exist in an $S = {}^3/_2 : S = {}^1/_2$ spin-state mixture and to be predominantly $S = {}^3/_2$ at 10 K. The Ni center is EPR silent and presumably Ni(II). X-ray absorption edge and EXAFS spectra reveal that the Ni center has a distorted square-planar geometry with two S donors at 2.19 Å and two N/O donors at 1.89 Å. Comparison of the Ni edge spectrum with those of structurally characterized $Ni(II)N_2S_2$ model compounds suggests a D_{2d} distortion with a dihedral angle of about 20–30°. The Ni center does not appear to be incorporated into the cluster, and it may or may not be bridged to the cluster. These centers may be decompositional relatives of the A-cluster, the active site for acetyl-coenzyme A synthesis.

Introduction

Carbon monoxide dehydrogenase from the acetogenic bacteria *Clostridium thermoaceticum* ($CODH_{Ct}$) catalyzes two types of reactions: the reversible oxidation of CO to CO_2 and the synthesis of acetyl coenzyme A (acetyl-CoA) from CO, a CO_2-derived methyl group, and coenzyme A. Acetyl-CoA is the starting material for various anabolic processes that allow acetogenic bacteria to grow autotrophically on CO_2 and H_2.[1,2] Besides $CODH_{Ct}$, acetyl-CoA synthesis requires a methyltransferase and a corrin-and-Fe_4S_4-containing enzyme (CoFeS) and is stimulated by a ferredoxin (FdII).[3] CoFeS transfers the methyl group to the active site in $CODH_{Ct}$.[1,2]

$CODH_{Ct}$ reportedly has an $\alpha_3\beta_3$ hexameric quaternary protein structure and a molecular mass of *ca.* 460 000 Da.[4] The α and β subunits have molecular masses of 81 730 and 72 928 Da, respectively.[5] Each αβ dimer contains, on average, 2 Ni, 11–13 Fe, and *ca.* 14 S^{2-} ions.[4,6] These ions are organized into four types of metal centers including the *A-cluster*,[7] the *C-cluster*, *ferrous component II* (FCII), and one or more $[Fe_4S_4]^{1+/2+}$ clusters.[6,8,9] The A-cluster is almost certainly the active site for acetyl-CoA synthesis.[10–14] It appears to consist of a Ni center exchange-coupled through a bridge to an Fe–S cluster.[6,15,16] The irons in the A-cluster have Mössbauer parameters typical of $[Fe_4S_4]^{2+}$ clusters.[6] The C-cluster contains Fe[6] and probably Ni and S, and it likely serves as the active site for CO oxidation.[14,17,18] FCII consists of a ferrous ion, but little else about it is known.[6] The Fe_4S_4 cluster(s) transfer(s) electrons between the C-cluster and external redox agents.[14,18]

The Ni environments are particularly interesting because there are so few naturally-occurring nickel-containing enzymes, and much Ni chemistry remains to be understood.[19] There are several types of Ni centers in $CODH_{Ct}$, including those associated with the A-cluster and the C-cluster. There also might be Ni ions in the enzyme that are not associated with either cluster.[13] The geometries and ligand environments of

[†] Texas A & M University.
[‡] University of Georgia.
[§] Present address: Department of Applied Science, Brookhaven National Laboratory, Upton, NY 11973.
* To whom correspondence should be addressed.
[⊗] Abstract published in *Advance ACS Abstracts,* June 15, 1995.

(1) Wood, H. G.; Ljungdahl, L. G. In *Variations in Autotrophic Life*; Shively, J. M., Barton, L. L. Eds.; Academic Press: London, 1991; pp 201–250.
(2) Ragsdale, S. W. *CRC Crit. Rev. Biochem. Mol. Biol.*,**1991**, *26*, 261–300.
(3) Roberts, J. R.; Lu, W.-P.; Ragsdale, S. W. *J. Bacteriol.* **1992**, *174*, 4667–4676.
(4) Ragsdale, S. W.; Clark, J. E.; Ljungdahl, L. G.; Lundie, L. L.; Drake, H. L. *J. Biol. Chem.* **1983**, *258*, 2364–2369.
(5) Morton, T. A.; Runquist, J. A.; Ragsdale, S. W.; Shanmugasundaram, T.; Wood, H. G.; Ljungdahl, L. G. *J. Biol. Chem.* **1991**, *266*, 23824–23828.
(6) Lindahl, P. A.; Ragsdale, S. W.; Münck, E. *J. Biol. Chem.* **1990**, *265*, 3880–3888.
(7) .The A-cluster was previously called "the NiFe Complex".
(8) Lindahl, P. A.; Münck, E.; Ragsdale, S. W. *J. Biol. Chem.* **1990**, *265*, 3873–3879.
(9) Shin, W.; Stafford, P. R.; Lindahl, P. A. *Biochemistry* **1992**, *31*, 6003–6011.
(10) Gorst, C. M., Ragsdale, S. W. *J. Biol. Chem.* **1991**, *266*, 20687–20693.
(11) Shin, W.; Lindahl, P. A. *Biochemistry* **1992**, *31*, 12970–12875.
(12) Shin, W.; Lindahl, P. A. *J. Am. Chem. Soc.* **1992**, *114*, 9718–9719.
(13) Shin, W.; Anderson, M. E.; Lindahl, P. A. *J. Am. Chem. Soc.* **1993**, *115*, 5522–5526.
(14) Kumar, M., Lu, W.-P., Liu, L.; Ragsdale, S. W. *J. Am. Chem. Soc.* **1993**, *115*, 11646–11647.
(15) (a) Ragsdale, S. W.; Ljungdahl, L. G.; DerVartanian, D. V. *Biochem. Biophys. Res. Commun.* **1983**, *115*, 658–665. (b) Ragsdale, S. W.; Wood, H. G.; Antholine, W. E. *Proc. Natl Acad. Sci. U.S.A.* **1985**, *82*, 6811–6814. (g) Fan, C.; Gorst, C. M.; Ragsdale, S. W.; Hoffman, B. M. *Biochemistry* **1991**, *30*, 431–435.
(16) Bastian, N. R.; Diekert, G.; Niederhoffer, E. C.; Teo, B. K.; Walsh, C. T.; Orme-Johnson, W. H. *J. Am. Chem. Soc.* **1988**, *110*, 5581–5582.
(17) Anderson, M. E.; DeRose, V. J.; Hoffman, B. M.; Lindahl, P. A. *J. Am. Chem. Soc.* **1993**, *115*, 12204–12205.
(18) Anderson, M. E.; Lindahl, P. A. *Biochemistry* **1994**, *33*, 8702–8711.
(19) Lancaster, J. R. Ed., *The Bioinorganic Chemistry of Nickel*; VCH: New York, 1988.

0002-7863/95/1517-7065$09.00/0

the Ni ions have been examined using X-ray absorption spectroscopy (XAS).[16,20] The XAS Ni edge of $CODH_{Ct}$ has a small feature at 8338 eV that arises from a 1s → $4p_z$+ shakedown transition and indicates distorted square-planar and/or trigonal-pyramidal geometries.[20] The Ni EXAFS fit best to an average (per Ni) of two to four S backscatterers at 2.16–2.21 Å and two to zero N/O scatterers at 1.97 Å.[20] There is some evidence for an Fe scatterer at 3.3 Å, which, if supported by additional studies, would indicate a Ni complex bridged to an Fe–S cluster.[16] Unfortunately, these results reflect the average Ni environment; the geometries and ligands of specific Ni sites remain somewhat obscure.

The number and properties of Fe_4S_4 clusters in the enzyme are also uncertain. The reduced enzyme exhibits two g_{av} = 1.94 EPR signals with similar g-values but different line widths.[8] Such signals are typical of $[Fe_4S_4]^{1+}$ clusters with $S = {}^1/_2$ spin states. Together, they quantify to only 0.64 ± 0.14 spin/$\alpha\beta$, significantly less than the 1 spin/$\alpha\beta$ expected if each $\alpha\beta$ contained one such cluster. The reduced enzyme also exhibits EPR features between $g = 6$ and 3, suggesting the presence of $[Fe_4S_4]^{1+}$ clusters with $S = {}^3/_2$ spin states. To explain the low EPR signal intensity and the presence of these low-field features, the clusters were considered to exist in an $S = {}^1/_2 : S = {}^3/_2$ spin-state mixture.[6] However, the absence of Mössbauer features typical of $S = {}^3/_2$ $[Fe_4S_4]^{1+}$ clusters suggested that the enzyme contained predominantly $S = {}^1/_2$ $[Fe_4S_4]^{1+}$ clusters. The Mössbauer components thought to originate from these clusters correspond to about one Fe_4S_4 cluster per $\alpha\beta$.[6] On the other hand, the magnitude of the oxidized-minus-reduced molar extinction coefficient in $CODH_{Ct}$ at 420 nm ($\Delta\epsilon_{420}$ = 14 700 cm^{-1} M^{-1}) is far greater than that expected for a single Fe_4S_4 cluster (*ca.* 6000 cm^{-1} M^{-1}).[9]

To eradicate these uncertainties in the number and types of metal centers present in the enzyme, we have endeavored to decompose native $CODH_{Ct}$ into subunits without disrupting the metal centers housed therein. We recently found that native $CODH_{Ct}$ treated with low concentrations of the detergent sodium dodecyl sulfate decomposes into α metallosubunits and a species composed primarily of β subunits.[21] The latter species has full CO oxidation activity, suggesting that the β subunits are involved in CO oxidation. This correlation is supported by the fact that the amino acid sequence of β is 46% identical to the monomeric CODH from *Rhodospirillum rubrum* ($CODH_{Rr}$).[22] $CODH_{Rr}$ catalyzes the reversible oxidation of CO to CO_2 but not the synthesis of acetyl-CoA. It contains one Ni and *ca.* six to eight Fe, organized into an active-site cluster analogous to the C-cluster of $CODH_{Ct}$, and an Fe_4S_4 cluster that exhibits g_{av} = 1.94 signals when reduced.[22–26] This correlation suggests that the C-cluster of $CODH_{Ct}$ is in the β subunit.

The α subunits are probably required for acetyl-CoA synthesis. They bind coenzyme A and two proteins involved in this activity (CoFeS and FdII).[27–31] The adenine portion of coenzyme A binds to α-tryptophan 418, while FdII docks in the region between residues α-229 and α-239. CoFeS binds *in vivo* using a disulfide bond to α-cysteine 506.[30] This cysteine is part of a cysteine-rich region that may be used for binding metal centers.[5] These considerations suggest that the A-cluster may be located in the α subunit.

To better evaluate the metal centers housed in α, we have prepared α in large quantities and characterized it spectroscopically. We report here that α contains a distorted square-planar Ni complex with two S and two N/O ligands and an $[Fe_4S_4]^{2+/1+}$ cluster with $S = {}^3/_2$ predominating in its reduced state.

Experimental Procedures

Cultures of *C. thermoaceticum* were grown, and two batches of $CODH_{Ct}$ were purified, as described.[32–36] Batches 1 and 2 had CO oxidation activities of 390 and 230 units/mg, and CO/acetyl-CoA exchange activities of 0.13 and 0.06 units/mg respectively. These batches of native enzyme were >90% pure according to SDS-PAGE.[37]

α was isolated anaerobically in an argon-atmosphere glovebox (Vacuum/Atmospheres model HE453) using a modification of a published procedure.[21] Degassed 6–7% polyacrylamide separating gel solution (8 cm), pH 8.8, and 3.3% stacking gel (1.5 cm), pH 6.8, were cast in the 37 mm diameter gel tube of a Bio-Rad model 491 preparative electrophoresis cell. To the separating and stacking gel solutions were added 15 and 5 μL of 1% w/v ammonium persulfate, respectively. Butanol was not used as a layering agent. The degassed electrode buffer in both upper and lower chambers and the elution buffer was 0.025 M Trisma base and 0.192 M glycine. Four samples from batch 1 (4 mL of 7.7 mg/mL) were each incubated in SDS (0.5 mL of 0.345 M) for 1 h at *ca.* 26 °C. One sample of batch 2 (2 mL of 6.2 mg/mL) was incubated similarly, except using 0.2 mL of SDS. Glycerol (1 mL of 80% v/v) and bromophenol blue (50 μL of 1% w/v) were then added. After the cell and buffers were cooled to 7–15 °C, samples were loaded and electrophoresed at 12 W constant power. Eluted fractions were collected at 0.74 mL/min, then assayed by SDS-PAGE. Those fractions containing only α were concentrated with a Centricon-30 (Amicon, Inc). The "as-isolated" samples were transferred to a double-septum-sealed quartz UV–vis cuvette, and spectra were collected (Perkin Elmer λ3B). Sodium dithionite (5 mM stock) was added until the absorbance at 420 nm ceased to decline beyond that due to dilution effects. The samples were transferred to EPR tubes and frozen for analysis (Bruker ESP300). Samples were then thawed, and portions were removed for protein (biuret[38]) and metal analyses. For metal analysis, samples were digested in 0.85 M metal-free nitric acid and subjected to graphite-furnace atomic absorption spectrophotometry (Perkin Elmer, model 2380). Absorbances were calibrated to metal concentrations by the standard curve method.

The remaining portions of these samples were combined, concentrated further, diluted with 50 mM potassium phosphate (pH 7), reconcentrated, and rediluted with glycerol (40% final concentration). Half (the "as-isolated" sample) was loaded into a 2 × 4 × 24 mm Lucite XAS cuvette with one 4 × 24 mm side covered by a 0.025 mm Mylar window, and half (the "dithionite-reduced" sample) was incu-

(20) Cramer, S. P.; Eidsness, M. K.; Pan, W.-H.; Morton, T. A.; Ragsdale, S. W.; DerVartanian, D. V.; Ljungdahl, L. G.; Scott, R. A. *Inorg. Chem.* **1987**, *26*, 2477–2479.
(21) Xia, J.; Lindahl, P. A. *Biochemistry* **1995**, *34*, 6037–6042.
(22) Kerby, R. L.; Hong, S. S.; Ensign, S. A.; Coppoc, L. J.; Ludden, P. W.; Roberts, G. P. *J. Bacteriol.* **1992**, *174*, 5284–5294.
(23) Bonam, D. Ludden, P. W. *J. Biol. Chem.* **1987**, *262*, 2980–2987.
(24) Ensign, S. A.; Hyman, M. R.; Ludden, P. W. *Biochemistry* **1989**, *28*, 4973–4979.
(25) Stephens, P. J.; McKenna, M.-C.; Ensign, S. A.; Bonam, D.; Ludden, P. W. *J. Biol. Chem.* **1989**, *264*, 16347–16350.
(26) Tan, G. O.; Ensign, S. A.; Ciurli, S.; Scott, M. J.; Hedman, B.; Holm, R. H.; Ludden, P. W.; Korszun, Z. R.; Stephens, P. J.; Hodgson, K. O. *Proc. Natl. Acad. Sci. U.S.A.* **1992**, *89*, 4427–4431.
(27) Shanmugasundaram, T.; Kumar, G. K.; Wood, H. G. *Biochemistry* **1988**, *27*, 6499–6503.
(28) Shanmugasundaram, T.; Kumar, G. K.; Shenoy, B. C.; Wood, H. G. *Biochemistry* **1989**, *28*, 7112–7116.
(29) Shanmugasundaram, T.; Wood, H. G. *J. Biol. Chem.* **1992**, *267*, 897–900.
(30) Shanmugasundaram, T.; Sundaresh, C. S.; Kumar, G. K. *FEBS Lett.* **1993**, *326*, 281–284.
(31) Lu, W.-P.; Ragsdale, S. W. *J. Biol. Chem.* **1991**, *266*, 3554–3564.
(32) Lundie, L. L., Jr.; Drake, H. L. *J. Bacteriol.* **1984**, *159*, 700–703.
(33) Ragsdale, S. W.; Wood, H. G. *J. Biol. Chem.* **1985**, *260*, 3970–3977.
(34) Ramer, S. E.; Raybuck, S. A.; Orme-Johnson, W. H.; Walsh, C. T. *Biochemistry* **1989**, *28*, 4675–4680.
(35) Raybuck, S. A.; Bastian, N. R.; Orme-Johnson, W. H.; Walsh, C. T. *Biochemistry* **1988**, *27*, 7698–7702.
(36) Shin, W.; Lindahl, P. A. *Biochim. Biophys. Acta* **1993**, *1161*, 317–322.
(37) Weber, K.; Osborn, M. *J. Biol. Chem.* **1969**, *244*, 4406–4412.
(38) Pelley, J. W.; Garner, C. W.; Little, G. H. *Anal. Biochem.* **1978**, *86*, 341–343.

Table 1. X-ray Absorption Spectroscopic Data Collection and Reduction for *C. thermoaceticum* CODH Samples

	Fe EXAFS	Ni EXAFS
SR facility	SSRL	SSRL
beamline	7-3	7-3
monochromator crystal	Si[220]	Si[220]
detection method	fluorescence	fluorescence
detector type	solid state array[a]	solid state array[a]
scan length, min	20	21
scans in average	4	12
temperature, K	10	10
energy standard	Fe foil (first inflection)	Ni foil (first inflection)
energy calibration, eV	7111.2	8331.6
E_0, eV	7130	8350
pre-edge background energy range, eV (polynomial order)	7200−7823 (2)[b]	8400−8973 (2)[b]
spline background energy range, eV (polynomial order)	7140−7250 (2) 7250−7500 (3) 7500−7823 (3)	8350−8520 (2) 8520−8750 (3) 8750−8973 (3)

[a] The 13-element Ge solid-state X-ray fluorescence detector at SSRL is provided by the NIH Biotechnology Research Resource. [b] Background was calculated from fitting this (EXAFS) region, then a constant was substracted so that the background matched the data just before the edge.

bated with sodium dithionite (2 mM final concentration) and loaded into another XAS cuvette. The cuvettes were frozen on a liquid-nitrogen-cooled aluminum block, quickly removed from the glovebox, immersed in liquid N_2, then capped and stored until XAS examination.

Ni and Fe XAS data were collected at the Stanford Synchrotron Radiation Laboratory (SSRL) with the SPEAR ring running at 3.0 GeV and *ca.* 70 mA average stored current. Other details of XAS data collection and reduction are provided in Table 1. Analysis of the EXAFS data was performed by our standard procedures[39] using the EXAFSPAK analysis software (courtesy of G. N. George). Theoretical scattering parameters[40] were used and values for ΔE° for each shell were determined by curve-fitting Ni−N, Ni−S, Fe−S, and Fe···Fe shells of structurally characterized model compounds and then not varied during the optimizations (see Table 2).

Three $Ni^{II}N_2S_2$ model compounds were examined by XAS for comparison of the X-ray absorption edge spectra. These compounds had varying amounts of a twist distortion from pseudo-square-planar (C_{2v}) symmetry as measured by the angle, Φ, between planes defined by N−Ni−S and N′−Ni−S′. M. Y. Darensbourg kindly supplied a sample of (BME-DACO)Ni^{II},[41] which is nearly square-planar (Φ = 0°). H. Toftlund provided a sample of the Ni(II) complex of the Schiff base ligand derived from 4-formyl-1,3,-dimethylpyrazol-5-thiol and 2,2′-diaminobiphenyl,[42] which approaches a pseudo-tetrahedral geometry (Φ = 77.4°). We refer to this complex herein as Ni(mpzdab). K. S. Murray supplied a sample of Ni(mbdab), a Ni(II) complex with a similar Shiff base ligand derived from 2-formylthiophenol and 2,2′-diaminobiphenyl,[42,43] which displays an intermediate twisted geometry with Φ = 14.4°. X-ray absorption spectra were collected on finely ground powders of these samples by transmission at 10, 200, and 4 K, respectively.

Results

Preparation and Characterization of α. Native $CODH_{Ct}$ was treated with SDS and electrophoresed as described in the Experimental Procedures. The α metallosubunit was the first brown fraction to elute from the electrophoresis cell. The samples of isolated α were >95% pure (no other bands were observed by SDS-PAGE) and were obtained in yields ranging from 33% to 55% of the α in the original native samples. Yield estimates would have been higher (probably >70%) if the α in side fractions had been included in the calculations. Isolated α was quite stable and could be handled in a manner similar to that used for native enzyme. The four samples of α that were analyzed for metals contained an average of 1.0 ± 0.1 Ni/α and 3.8 ± 0.3 Fe/α.

Electronic Absorption Spectra of α. "As-isolated" α exhibited a shoulder in the 400 nm region (Figure 1, solid line) that declined in intensity when the reductant dithionite was added (Figure 1, dashed line). $\Delta\epsilon_{420}$ for α corresponded to 4000 M^{-1} cm^{-1}. The energy, shape, and redox-dependent changes associated with this shoulder suggest that it arises from Fe_4S_4 clusters. The spectral intensity did not increase when the oxidant thionin was added, indicating that the chromophore was fully oxidized in the "as-isolated" state. These results provide the first evidence that the four irons in α are organized into an

Table 2. Curve-Fitting Results for Ni and Fe EXAFS of *C. thermoaceticum* CODH[a]

sample	fit	shell	N_s	R_{as} (Å)	σ_{as}^2 (Å^2)	ΔE_0 (eV)	f'[b]
α, subunit, as isolated (Ni EXAFS)	1	Ni−N	(4)[c]	2.00	0.0073	(−3.0)	0.208
	2	Ni−N	(3)	1.92	0.0081	(−3.0)	0.074
		Ni−S	(1)	2.20	−0.0008[d]	(−5.9)	
	3	Ni−N	(2)	1.89	0.0063	(−3.0)	0.058
		Ni−S	(2)	2.19	0.0025	(−5.9)	
	4	Ni−N	(1)	1.85	0.0015	(−3.0)	0.059
		Ni−S	(3)	2.18	0.0051	(−5.9)	
	5	Ni−S	(4)	2.18	0.0080	(−5.9)	0.098
α subunit, reduced (Ni EXAFS)	6	Ni−N	(4)	1.98	0.0088	(−3.0)	0.200
	7	Ni−N	(3)	1.92	0.0070	(−3.0)	0.067
		Ni−S	(1)	2.20	−0.0007	(−5.9)	
	8	Ni−N	(2)	1.89	0.0050	(−3.0)	0.052
		Ni−S	(2)	2.19	0.0027	(−5.9)	
	9	Ni−N	(1)	1.86	0.0008	(−3.0)	0.054
		Ni−S	(3)	2.18	0.0054	(−5.9)	
	10	Ni−S	(4)	2.18	0.0086	(−5.9)	0.097
α subunit, as isolated (Fe EXAFS)	11	Fe−S	(4)	2.30	0.0038	(−5.0)	0.036
		Fe−Fe	(3)	2.71	0.0038	(−14.2)	
α subunit, reduced (Fe EXAFS)	12	Fe−S	(4)	2.30	0.0044	(−5.0)	0.043
		Fe−Fe	(3)	2.72	0.0041	(−14.2)	

[a] N_s is the number of scatterers per metal. R_{as} is the metal-scatterer distance. σ_{as}^2 is a mean square deviation in R_{as}. ΔE_0 is the shift in E_0 for the theoretical scattering functions. All fits were performed over the range k = 2−12.5 Å^{-1}. [b] f' is a normalized error (χ-squared):

$$f' = \frac{\{\sum_i [k^3(\chi_{obs}(i) - \chi_{calcd}(i))]^2/N\}^{1/2}}{[k^3(\chi_{max} - \chi_{min})]}$$

[c] Numbers in parentheses were not varied during optimization. [d] Underlined values are physically or chemically unreasonable.

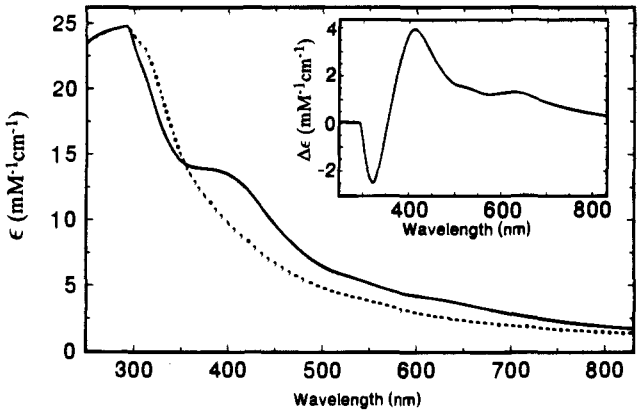

Figure 1. Electronic absorption spectra of thionin-oxidized α (solid line) and dithionite-reduced α (dashed line). Inset: oxidized-minus-reduced difference spectrum. Sample was 73 μM, batch 2.

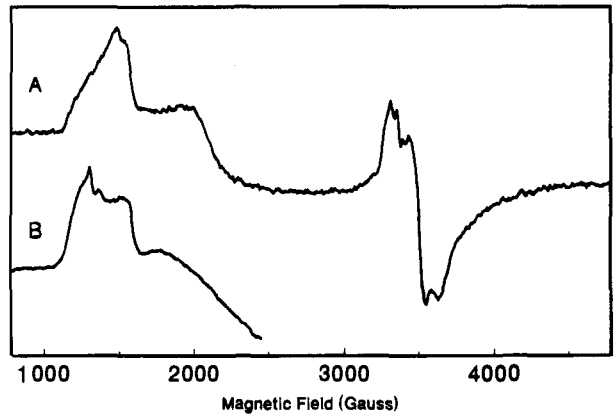

Figure 2. EPR of α (A) and native $CODH_{Cl}$ (B). Sample characteristics: α (190 μM, 2 mM dithionite, batch 1); native (186 μM αβ, 2 mM dithionite, and 1 atm CO; 230 units/mg CO oxidation activity, 0.21 units/mg CO/acetyl-CoA exchange activity). EPR conditions for A: microwave frequency, 9.429 GHz; microwave power, 0.05 mW; sample temperature, 10 K; modulation amplitude, 20 G; sweep time, 167 s; time constant, 0.327 s. EPR conditions for B were the same except for the following: microwave frequency, 9.450 GHz; microwave power, 63 mW; time constant, 1.3 s.

Fe_4S_4 cluster. We will call this cluster the α-*Fe_4S_4* cluster. The $\Delta\epsilon_{420}$ value for α was only a fraction of that obtained for native enzyme (measured on a per αβ molar basis), suggesting that, besides α-Fe_4S_4, native αβ units contain at least one other chromophore that contributes to the total changes at 420 nm. Oxidized α also exhibited very minor features at 530 and 625 nm (Figure 1, inset). These features were less pronounced in the spectrum of dithionite-reduced α, suggesting that they originate from a redox-active chromophore. We considered that they were due to the Ni, but other results (see below) indicate that this center is redox inactive within the potential range examined. Thus, these features remain unassigned.

Electron Paramagnetic Resonance of α. Dithionite-reduced α exhibited relatively strong EPR features between $g = 6$ and 3, and a weak $g_{av} = 1.94$-type signal ($g = 2.04, 1.93, 1.86$), quantifying to only 0.1 spin/α (Figure 2A). The low-field features have shapes and g-values similar to, but not the same as, those from native enzyme (Figure 2B). These features suggest that the $[Fe_4S_4]^{1+}$ cluster in α has an $S = {}^3/_2$, $S = {}^1/_2$ spin-state mixture. The best-characterized cluster exhibiting such a spin-state mixture is in the Fe protein of nitrogenase. At 10 °C, 40% of the nitrogenase Fe protein clusters are $S = {}^1/_2$ and yield $g_{av} = 1.94$ EPR signals; the remainder are $S = {}^3/_2$ and yield features between $g = 6$ and 4.[44,45] The proportion of each spin-state varies depending on the solvent. α-$[Fe_4S_4]^{1+}$

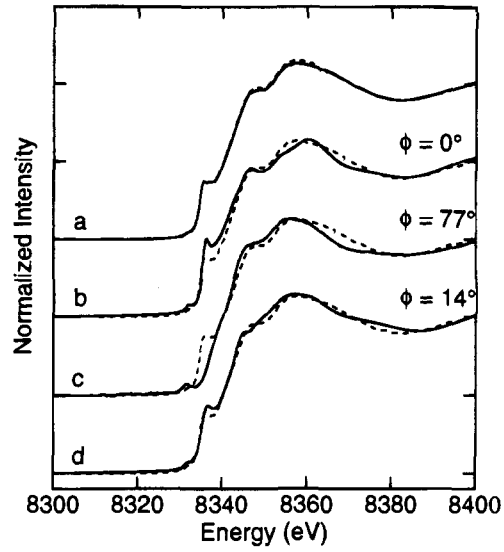

Figure 3. Ni X-ray absorption edge spectra of CODH α metallosubunit and Ni(II) model compounds: (a) as-isolated (solid) and dithionite-reduced (dashed) α metallosubunit; (b–d) as-isolated α metallosubunit (dashed) compared with (BME-DACO)Ni(II), (c) Ni(mpzdab), and (d) Ni(mbdab) (all solid). Φ is the dihedral angle between planes defined by N–Ni–S and N′–Ni–S′.

appears to be predominantly $S = {}^3/_2$, given the low spin intensity of the $g_{av} = 1.94$ signal. Both as-isolated and thionin-oxidized α were EPR-silent, indicating that the cluster in these forms was in the 2+ core oxidation state. Neither oxidized nor dithionite-reduced α exhibited EPR signals attributable to the Ni center. This suggests that the Ni is redox-inactive and in the Ni(II) state, at least within the potential range examined.

X-ray Absorption Spectra of α. Shown in Figure 3a is the Ni X-ray absorption edge spectrum of as-isolated (solid line) and dithionite-reduced α (dashed line). The spectra have fairly strong features at 8338 eV, arising from the 1s → $4p_z$+ shakedown transition.[46] Such transitions are most intense in square-planar complexes, least intense in tetrahedral ones.[39,47] For a four-coordinate complex NiL_2X_2, the dihedral angle Φ formed by the L–Ni–X and L′–Ni–X′ planes varies from 0° (square-planar) to 90° (tetrahedral). Ni X-ray absorption edge spectra for $Ni(II)N_2S_2$ complexes with varying values of Φ are compared with the spectra of as-isolated α in Figure 3b–d. As Φ varies from 0° (Figure 3b) to near 90° (Figure 3c), the 8338 eV transition disappears and the intensity of the 1s → 3d transition near 8332 eV increases. The size of the 8338 eV transition in the Ni edge spectrum of α suggests an intermediate geometry, slightly more distorted than the Ni(II) compound represented in Figure 3d (Φ = 14°). We estimate that Φ = 20–30° for the Ni(II) site in α. The Ni X-ray absorption spectrum of dithionite-reduced α was similar to that of as-isolated α (Figure 3a), providing further evidence that the Ni center is redox-inactive. The Fe XAS edge of α (data not shown) was typical of Fe_4S_4 clusters and was not analyzed further.

Shown in Figure 4 are the background-removed Ni EXAFS of as-isolated α (solid line in a), the corresponding Fourier-transform (solid line in b), the Fourier-filter window (dotted

(39) Scott, R. A. *Methods Enzymol.* **1885**, *117*, 414–459.
(40) McKale, A. G.; Veal, B. W.; Paulikas, A. P.; Chan, S.-K.; Knapp, G. S. *J. Am. Chem. Soc.* **1988**, *110*, 3763–3768.
(41) Mills, D. K.; Reibenspies, J. H.; Darensbourg, M. Y. *Inorg. Chem.* **1990**, *29*, 4364–4366.
(42) Frydendahl, H.; Toftlund, H.; Becher, J.; Dutton, J. C.; Murray, K. S.; Taylor, L. F.; Anderson, O. P.; Tiekink, E. R. T. *Inorg. Chem.* **1995**, *34*, in press.

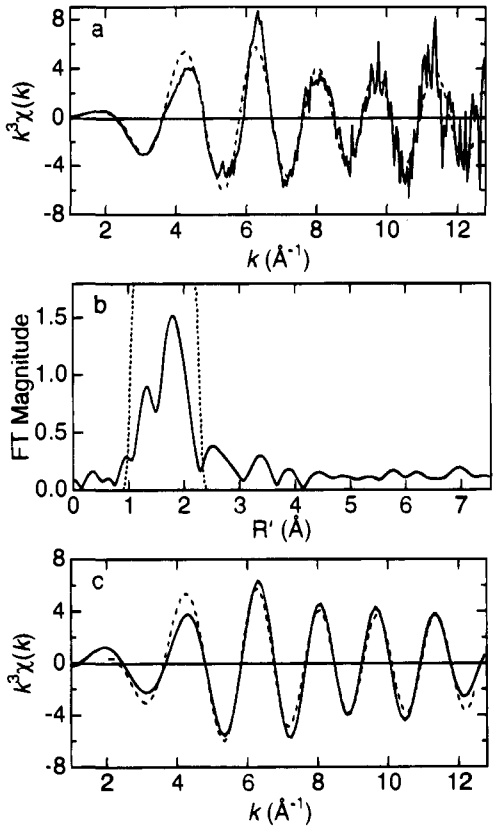

Figure 4. Ni EXAFS and Fourier transform of as-isolated α metallosubunit. Background-removed Ni EXAFS data, multiplied by k^3, (solid line in a) were transformed over the k = 1−12.5 Å^{-1} range to yield the FT (solid line in b). The first-shell FT peaks were filtered using a Gaussian window (dotted line in b) and back-transformed to yield the first-shell filtered EXAFS data (solid line in c). Curve fitting of these data yielded the best-fit simulation from fit 3 in Table 2 (dashed lines in c and a).

line in b), and the Fourier-filtered EXAFS (solid line in c). The spectra for dithionite-reduced α were virtually identical (data not shown). Fourier-filtered EXAFS data were simulated as described in the Experimental Procedures with either one or two backscattering terms, and the parameters from these fits are given in Table 2. In no case did the addition of a third backscattering term improve the best two-term fit. For both as-isolated and dithionite-reduced α, a one-term fit to a NiS_4 coordination (fits 5 and 10 in Table 2) was significantly improved (by 1.7−1.9 times) by adding a second shell of N backscatterers. For the two-shell NiN_xS_y fits, best-fit values of x and y were 2 and 2, and best-fit Ni−N and Ni−S distances were 1.89 and 2.19 Å, for both samples (fits 3 and 8). Although NiN_1S_3 fits gave nearly equivalent values of f' (goodness of fit), the Debye−Waller σ_{as}^2 values for the Ni−N interaction were smaller than observed in any model compound we have examined. We conclude that the Ni in as-isolated and dithionite-reduced α is ligated by two S donors (probably cysteine thiolates) and two N/O donors (probably histidine, aspartate, and/or glutamate residues). The identical Ni site structures deduced in both as-isolated and reduced forms of α provide

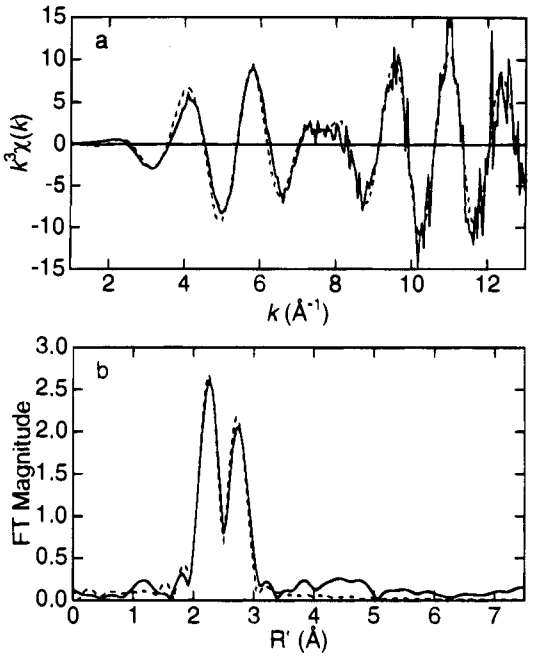

Figure 5. Fe EXAFS and Fourier transform of as-isolated α metallosubunit. Background-removed Fe EXAFS data, multiplied by k^3 (solid line in a) were transformed over the k = 1−12.5 Å^{-1} range to yield the FT (solid line in b). Curve fitting of the raw Fe EXAFS data yielded the best-fit simulation from fit 11 of Table 2 (dashed line in a) and its FT (dashed line in b).

further evidence that the Ni center is redox-inactive, at least between the potentials probed, and that its geometry does not change with potential. We also attempted to fit the data with Fe backscatterers at 2.7 or 3.2 Å, but this yielded no positive evidence for a Ni···Fe interaction. Considering the substantial difficulties involved, we can exclude the possibility that the Ni center is incorporated into the corner of an Fe−S cluster but cannot exclude it being bridged to the cluster.

Fe EXAFS data and curve-fitting results are shown in Figure 5 and Table 2. In this case, no Fourier filtering was performed; the background-removed EXAFS data themselves were fit. The irons in α, on average, have four S donors at 2.3 Å, and three irons at 2.7 Å (fit 11). The EXAFS data and analysis provide further evidence that the irons in α subunits are organized into Fe_4S_4 clusters. They also suggest that the predominant ligands holding the cluster into α are S-donors (probably cysteines). The uncertainty in these results allows for the possibility of one or two N/O donor ligands per cluster (but there is no evidence supporting this). No significant differences in bond lengths were observed when the cluster was reduced (Table 2). This insensitivity to redox-state changes is commonly observed in the XAS spectra of Fe_4S_4 clusters, since the electron used in reduction delocalizes throughout the cluster. The redox activity of the cluster is better assessed by EPR and electronic absorption spectroscopy.

Discussion

The results presented here demonstrate conclusively that α metallosubunits, when separated from the native enzyme, contain a Ni center and an $[Fe_4S_4]^{2+/1+}$ cluster. The Ni is ligated by two S (probably cysteines) and two N/O donors, in a distorted square-planar geometry, with a dihedral angle of *ca.* 20°−30°. Between potentials of *ca.* +0.1 and −0.6 V *vs* NHE, the Ni is redox-inactive and in the Ni(II) oxidation state. The Fe_4S_4 cluster is probably ligated by four cysteine ligands and can access the 2+ and 1+ core oxidation states. In the reduced

(43) Murray, K. S. Unpublished work.
(44) Lindahl, P. A.; Day, E. P.; Kent, T. A.; Orme-Johnson, W. H.; Münck, E. *J. Biol. Chem.* **1985**, *260*, 11160−11173.
(45) Lindahl, P. A.; Gorelick, N. J.; Münck, E.; Orme-Johnson., W. H. *J. Biol. Chem.* **1987**, *262*, 14945−14953.
(46) Kosngi, N.; Yokoyama, T.; Asakura, K.; Kuroda, H. *Chem. Phys.* **1984**, *91*, 249−256.
(47) Eidsness, M. K.; Sullivan, R. J.; Scott, R. A. In *The Bioinorganic Chemistry of Nickel*; Lancaster, J., Ed.; VCH Publishers: New York, 1988; Chapter 4.

state at 10 K, the majority of clusters appear to be $S = {}^3/_2$ and exhibit EPR features between $g = 6$ and 3, while a small proportion (~10%) are $S = {}^1/_2$ and exhibit $g_{av} = 1.94$ EPR signals. Although the Ni is probably not incorporated into a corner of the cluster, it may be linked to the cluster via bridging ligands or it may be structurally and functionally independent of the cluster. These centers are probably bound within the "cysteine-rich" region of the α subunit, which extends from cysteine 506 to cysteine 608 and houses eight of the subunit's 10 cysteines.[5]

We are presently unable to determine whether the α subunit, when part of the native enzyme, contains additional metal centers that are lost during isolation. However, isolated α is very stable and contains near-integer values of metal ions; such properties certainly do not suggest metal loss. Also unknown is whether separating α from native enzyme alters the geometry or ligands of the Ni center or the relationship between the Ni center and the cluster. The magnetic properties of the $[Fe_4S_4]^{1+}$ cluster do appear to have changed, since the low-field EPR features due to the $S = {}^3/_2$ spin state of the cluster in isolated α differ from the EPR features of native enzyme.

If the geometry of the α-Ni center is assumed unchanged during isolation of α, the average geometry of the other Ni centers in native enzyme can be estimated. The 8338 eV Ni edge feature in the XAS Ni spectrum of native enzyme[20,47] is less intense than the same feature in the spectrum of isolated α. This suggests that the other Ni centers in native enzyme lack such a feature and have different geometries than the α-Ni. The XAS edge spectrum of the Ni center in $CODH_{Rr}$ also lacks the 8338 eV feature and has a stronger 1s → 3d transition at 8333 eV.[26] This pattern suggests a distorted five-coordinate or tetrahedral geometry. The EXAFS of this center fit best to two to three N at 1.87 Å and two S at 2.23 Å. The Ni in $CODH_{Rr}$ is probably Ni(II) and not incorporated into an Fe−S cluster. Given the apparent relation between β and $CODH_{Rr}$ (see the Introduction), the other Ni center of $CODH_{Ct}$ is probably in β, and it probably has a coordination environment similar to that in $CODH_{Rr}$.

If the number of irons in α is assumed unchanged during isolation, and metal ions are assumed not to be bound at subunit interfaces, the number of irons in β can be estimated. Given that each αβ dimer of $CODH_{Ct}$ contains 11−13 Fe, β would appear to contain seven to nine Fe. This estimate is within error of the observed iron content of $CODH_{Rr}$ (six to eight Fe), further supporting the proposed relationship of β to $CODH_{Rr}$. We have attempted to isolate β and determine its metal content, but it was unstable and tended to self-associate. The fractions obtained contained only 1.5−3.3 Fe/β and little Ni, suggesting substantial metal loss during isolation.

Since α in native enzyme appears to function in acetyl-CoA synthesis, and the A-cluster is almost certainly the active site for this activity, the Ni and Fe_4S_4 centers in isolated α may be decompositional relatives of this cluster. Further studies are required to determine whether this is so, but the presence in α of the two previously proposed components of the A-cluster[6] (i.e., a Ni center and an Fe_4S_4 cluster) certainly supports this possibility.

Acknowledgment. We thank M. Y. Darensbourg, K. S. Murray, and H. Toftlund for their kind gifts of model compounds used in the comparisons of Figure 3, Woonsup Shin for collecting the EPR spectrum of native $CODH_{Ct}$, and the National Institutes of Health (GM46441, P.A.L.; GM42025, R.A.S.) for financial support. The XAS data were collected at the Stanford Synchrotron Radiation Laboratory (SSRL), which is operated by the Department of Energy, Division of Chemical Sciences. The SSRL Biotechnology Program is supported by the National Institutes of Health, Biomedical Resource Technology Program, Division of Research Resources. Support for the X-ray fluorescence detector is from NIH BRS Shared Instrumentation Grant RR05648. The work done at the University of Georgia is (partially) supported by the NSF Research Training Group Award to the Center for Metalloenzyme Studies (DIR 90-14281).

JA950685G